Correlation of the electrical properties of metal contacts on diamond films with the chemical nature of the metal-diamond interface. I. Gold contacts: A non-carbide-forming metal

T. Tachibana, B. E. Williams, and J. T. Glass
Department of Materials Science and Engineering, Research Building I, Centennial Campus, North Carolina State University, Raleigh, North Carolina 27695-7919

(Received 17 July 1991; revised manuscript received 3 December 1991)

The gold–polycrystalline-diamond interface has been characterized by x-ray-photoelectron-spectroscopy (XPS), Auger-electron-spectroscopy (AES), and current-voltage (I-V) measurements. The I-V characteristics of gold contacts on polycrystalline diamond were correlated with interface observations by XPS and AES. Minimal interaction between the gold and diamond due to the inert nature of both materials led to the formation of rectifying contacts. Various predeposition treatments of the diamond including vacuum annealing, wet chemical cleaning, and argon sputtering were also examined. Predeposition vacuum annealing desorbed some of the physisorbed oxygen from the diamond surface. The wet chemical cleaning effectively removed nondiamond carbon. However, these treatments did not influence the interaction between the gold and polycrystalline diamond. Also, there was no difference in the I-V characteristics between the gold contacts on the treated diamond surface and those on the nontreated surface. Argon sputtering cleaned the diamond surface but created a damaged surface layer which appeared to be graphitic. As-deposited gold formed Ohmic contacts on the sputtered surface due to the presence of the damaged layer. Once annealed, however, these contacts became rectifying probably because the damaged layer was absorbed into the gold overlayer.

I. INTRODUCTION

Diamond is generally recognized as an insulating material. Once successfully doped, however, it is a superior wide-band-gap semiconducting material with a unique combination of properties such as high breakdown voltage, high thermal conductivity, small dielectric constant, and excellent radiation hardness. Therefore, it is considered a potentially useful active electronic device material for high-power, high-temperature, and harsh-environment applications. The exploration of possible electronic-device applications for this material has been motivated by this potential combined with the significant advances in growth processes accomplished over the past decade. In fact, active device fabrication attempts have been reported on both bulk and thin-film boron-doped diamond with some success.[1–4]

Obtaining high-quality contacts is one of the most frequently encountered problems in the development of materials for electronic-device applications. The properties of such electrical contacts directly contribute to the active device performance and thereby determine the commercial importance of a device. Bell and Leivo[5] observed rectifying characteristics for various kinds of metal point contacts. The barrier height of different metal contacts on single-crystal diamond has been measured using various techniques including C-V, I-V,[6] internal photoemission,[7] and photoelectron spectroscopy.[8] The reported values of barrier height are all in the range of 1.5–2 eV, independent of the metal. It has been considered that the Fermi level is strongly pinned at the diamond surface by a high density of surface states. Thus, rectifying contacts have been obtained via less reactive materials such as gold on moderately doped, undamaged diamond.[3,6,9–11]

On the other hand, it has been difficult to fabricate a good Ohmic contact on diamond due to its inert and wide-band-gap nature. It is necessary to somehow modify the nature of the perfect diamond surface. Several different methods have been examined to obtain Ohmic contacts on diamond. Reasonably good contacts have been formed by choosing or intentionally creating damaged surfaces.[12] Damaging includes the mechanical roughing of a surface which creates a high electric field between the metal and diamond, as well as creating a surface layer via particle bombardment which includes nondiamond carbon. This type of damage can make diamond remarkably conductive.[13] This is a useful method of obtaining Ohmic contact to diamond as long as (1) the damage is shallow, (2) the annihilation of damage is not intensive, and (3) the adhesion between the metal and damaged diamond is satisfactory. The last condition is very difficult to satisfy when a graphite layer is formed. Prins obtained Ohmic contacts to diamond which was highly doped by ion implantation.[14] Heavy doping of a semiconductor surface is the most commonly used method to obtain Ohmic contacts in silicon technology. It is necessary to thoroughly study the implantation and diffusion of dopants in diamond to adapt this method to device fabrication processes in a reliable manner. Another alternative reported is the use of carbide-forming metals such as titanium, molybdenum, and tantalum.[9,12,15–18] The Ohmic behavior of these metal contacts after annealing was attributed to the formation of carbide at the interface. The carbides are reliable con-

tacts as well as good diffusion barriers especially for high-temperature devices. Because it is even more difficult to control ion implantation doping in polycrystalline diamond than in single crystals, obtaining Ohmic contacts by carbide formation is an attractive method worth further study.

A variety of metal-diamond contacts have been electrically characterized. However, there have been few studies so far to reveal the basic mechanisms of contact formation in the metal-diamond system. The present study of interactions between metals and diamonds is intended to provide possible explanations of the electrical properties of contacts on diamond. Gold was selected as a contact metal representing the non-carbide-forming metals. There has been no report of "gold carbide" formation to our knowledge. On the other hand, titanium is a strong carbide former and has been reported to form Ohmic contacts after annealing.[9,15–18] These metals were carefully deposited via thermal evaporation in an ultrahigh-vacuum environment to exclude extrinsic factors such as substrate damaging and heating which might influence the metal-diamond interaction. I-V measurements on the metal contacts on diamond were combined with surface analytical characterization by x-ray photoelectron spectroscopy (XPS) and Auger-electron spectroscopy (AES) to probe the metal-diamond interface. This interfacial region is the factor which determines metal-contact properties on semiconductors.[19,20] This study is intended to be a helpful guide for systematically establishing the factors which determine the contact properties on diamond and for the selection of promising metallization material for diamond device fabrication.

II. EXPERIMENT

Boron-doped polycrystalline diamond films were grown by microwave plasma chemical-vapor deposition (CVD). The silicon substrates (n type, with resistivity of 10^3 Ω cm or greater) were polished with one-quarter micrometer diamond paste. The substrate was kept at 800 °C during the growth from methane, hydrogen, and diborane. Detailed information about the growth system has been described in Ref. 21. All the diamond films were observed in a scanning electron microscope (SEM). It was confirmed that the films were continuous and that there were no pinholes that could distort the results of the I-V measurements and the characterization of the gold-diamond interface via XPS and AES.

All the diamond samples in this study were grown *ex situ* though *in vacuo* growth is now possible with the integrated vacuum system described in the Appendix. The metal-diamond interface analysis was conducted *in vacuo* as described in the following paragraphs. Prior to their introduction into the system through a load lock, the samples were ultrasonically cleaned in trichloroethylene, acetone, and methanol, rinsed with deionized water, and then dried with nitrogen.

Gold was evaporated ~10 cm from the sample surface by resistively heating a tungsten filament around which gold wire (99.999% purity) was coiled. The base pressure of the system was $\sim 1\times 10^{-8}$ Torr and the pressure was kept in the 10^{-8}-Torr range during the deposition. This evaporation system was connected directly to the analysis system as described in the Appendix. The gold-overlayer thickness was determined by measuring the XPS peak area ratio of the Au $4f$ overlayer signal to the Si $2p$ signal from a silicon substrate placed adjacent to the diamond samples.[22] The sensitivity factor of pure gold was 14 times greater than that of pure silicon for the present system. Since clusters were observed in the early stages of the gold-overlayer formation via SEM, "equivalent thickness" in Å are used to indicate the coverage in this study.

The analytical system has a base pressure of 1×10^{-10} Torr. A RIBER MAC2 semi-imaging-type electron energy analyzer[23] concentric about the sample normal was used for both XPS and AES. The energy resolution, which is constant for this type of analyzer, was set at 1.1 eV as determined from the full width at half maximum of the $4f_{7/2}$ peak of pure gold. The sample surface was impinged at 75° from the sample normal by nonmonochromatized magnesium $K\alpha$ radiation and data were collected in the pulse counting mode for XPS. For AES, a 3-keV, $\sim 10^{-5}$-A electron beam directed 75° from the sample normal was used and the data were collected in the differentiated mode.

Since the C_{KLL} Auger peaks overlap the Auger signal of gold as shown in Sec. III, it was necessary to subtract the latter to observe changes in the diamond surface. There is no question that signals collected in the differentiated mode are more difficult to quantitatively analyze than those obtained in the integrated mode. However, the poor signal-to-noise ratio of Auger data obtained in the integrated mode using the present system caused us to acquire Auger data in the differentiated mode and to integrate numerically. The gold-overlayer signal was subtracted according to the thickness in the following manner: (1) A standard spectrum for a thick (~2000 Å) overlayer deposit of gold was obtained. (2) The Auger data collected in the differentiated mode for the diamond with a thin (a few Å) gold overlayer as well as the standard spectrum of the gold overlayer were numerically integrated. (3) The linear background signal was subtracted. (4) Since the equivalent thickness of the thin gold overlayer was known from XPS core-level intensity ratios, the Auger-signal intensity ratio of the gold overlayer versus the diamond substrate was calculated.[22] (5) The standard Auger signal of the overlayer was subtracted from the data of the diamond with the thin overlayer according to the ratio calculated in (4). (6) The data were numerically differentiated back to show the fine structure clearly. For this data manipulation, data from a single-crystal diamond with the same amount of gold overlayer were used to exclude the roughness of the polycrystalline-diamond surface.

Some samples were cleaned in a 3:4:1 solution of sulfuric, nitric, and perchloric acids heated to ~80 °C to remove nondiamond carbon on the surfaces as a predeposition treatment. The pre- and postdeposition annealings were conducted at a vacuum of less than 10^{-7} Torr and the sample temperature was measured using an infrared pyrometer. Predeposition argon sputtering of the diamond surface was also conducted *in vacuo* with an ac-

celeration voltage of 2 kV and an incident angle of ~65° from the surface normal.

The same evaporation system was used to deposit the gold overlayer for the *I-V* measurements. Initially, gold was deposited at the rate of ~0.4 Å/min, the same deposition rate used for XPS and AES analyses. After establishing the metal-diamond interface characteristics, the deposition rate was increased to 200 Å/min by increasing the filament current to obtain a thick (~2000 Å) overlayer. The samples were then taken out of the vacuum system to fabricate the contact patterns and to conduct *I-V* measurements. Circular 100-μm-diam active contacts separated from the field region by a 100-μm-wide concentric ring were defined by photolithography and the subsequent etching of gold in a 4:1:40 solution of potassium iodide, iodine, and deionized water. The *I-V* characteristics were obtained between the active contacts and the field region using a HP 4145B semiconductor parameter analyzer.

III. RESULTS AND DISCUSSION

A. Electrical properties

The *I-V* characteristics of gold contacts on boron-doped polycrystalline diamond thin films are shown in Fig. 1. As-deposited gold contacts on diamond are rectifying as previously reported.[6,9–11] The leakage current at a 5-V reverse bias is 3.4 μA. These contacts were subsequently annealed in vacuum for 30 min at 140 and 280 °C, respectively. After annealing, the leakage current for the 5-V reverse bias increased by a factor of 2 but the contacts remained rectifying. This result is similar to the characteristics of annealed gold contacts on diamond reported in the literature.[6,9–11]

B. Interface analyses of gold coverage series

In vacuo surface analyses were utilized to study the gold-diamond interface by interrupting the gold deposition and transferring the sample in vacuum to an analytical system. This information was then compared to the *I-V* characteristics which were obtained from samples prepared under similar conditions. As discussed later, this has allowed the development of a basic interface model.

The XPS C 1*s* peaks of polycrystalline diamond with various gold-overlayer coverages (Fig. 2) were utilized to evaluate the development of the interface characteristics. The peak was composed of signals from diamond as well as those from carbon contamination in the gold overlayer. The latter has a peak position which is 0.03-eV lower in binding energy than the diamond peak because of the charge redistribution predicted from Pauling's electronegativity difference between carbon (2.5) and gold (2.4). The signals from carbon contamination (shown as the dashed lines in Fig. 2) were subtracted according to their contribution (the result is the solid line in Fig. 2) which was determined as follows. The intensity ratio of Au 4*f* to C 1*s* was measured for the gold deposited on a carbon-free substrate (i.e., an argon-sputtered silicon). Using the sensitivity factor ratio (Au 4*f* to C 1*s*) of 4.0 for the spectrometer used in the present study, the carbon concentration in the gold was determined. From this experimental result, the contributions of carbon contamination in the gold to the C 1*s* peak from 1.5, 3.4, and 4.9 Å equivalent thicknesses, were calculated to be 1.6%, 3.7%, and 5.5%, respectively, using Fadley's overlayer model.[22]

The binding energy of the C 1*s* peak from diamond was set at 284.6 eV to correct for charging effects which were observed from sample to sample. The peak position of the gold may not be used to correct for charging since it can deviate by as much as 1 eV from its bulk state position when the gold is in the form of small clusters.[24] The peaks illustrated in Fig. 2 were normalized to the same height for comparison. In actuality, the intensity of the C 1*s* peak was attenuated as the gold-overlayer thickness increased. There was no change observed in the peak shape nor in the peak width. This result excludes the possibility that "gold carbide" was formed. A similar result was obtained for the valence-band spectrum which

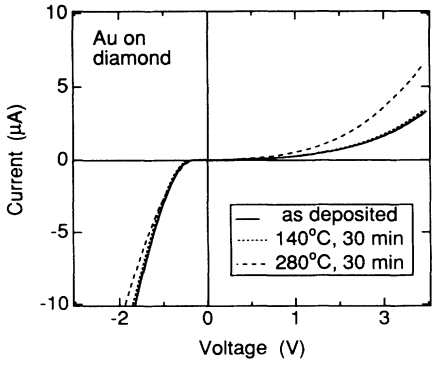

FIG. 1. *I-V* characteristics of gold contacts on boron-doped polycrystalline diamond grown by microwave plasma chemical-vapor deposition on silicon.

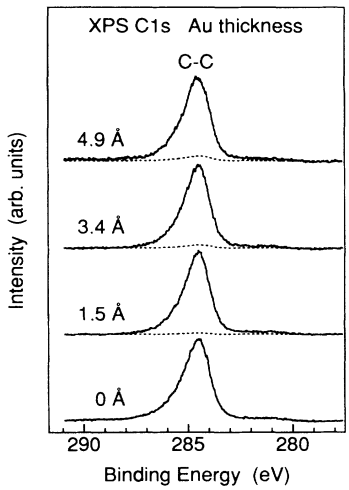

FIG. 2. XPS C 1*s* peaks of boron-doped polycrystalline diamond at various gold coverages after subtraction of carbon contamination (dashed lines indicate signals from carbon contamination in gold overlayer).

indicates the absence of interaction between gold and diamond. The polycrystalline diamond in the present research showed three peaks (2*s*, 2*s*-2*p*, and 2*p*) with a characteristic combination of intensity ratios as was observed for single-crystal diamond by McFeely and coworkers.[25] As the gold coverage increased, the Au 5*d* peaks became dominant and the diamond features diminished.

These XPS results confirmed that no carbide-forming reaction occurred during the process of gold deposition. However, the possibility of the transformation of diamond to another pure form of carbon (i.e., graphite, amorphous carbon, etc.) could not be excluded since all pure carbons have the same binding energy for the C 1*s* peak[26] within the resolution of the spectrometer used in the present research, and the valence-band spectra were not clear enough due to the presence of the gold overlayer to determine the bonding state of the carbon. Thus, this possibility was examined more clearly via Auger fine-structure observations since the C_{KLL} peak has a characteristic shape reflecting the bonding state of carbon.[27] Since gold and diamond have overlapping Auger peaks in this region of kinetic energy and since carbon contamination codeposited with the gold can also affect the fine structure, these overlapping peaks from the gold and codeposited carbon contamination were subtracted in the integrated form of the spectra according to the equivalent thickness, as described in detail in the experimental procedures. The subtracted spectra, which reflect the Auger signal from the diamond surface, are shown in Fig. 3.[28] The fine structure remains that of diamond after the gold deposition. This analysis also supports the lack of interaction between the diamond and gold.

There were several assumptions used in the subtraction which should be mentioned. The background was assumed to be linear for the Auger electrons. This was found to be the most reliable in terms of reproducibility and consistency compared to other background fitting routines such as the polynomial and Shirley methods.

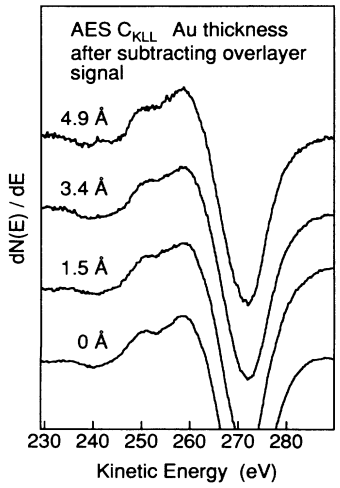

FIG. 3. C_{KLL} Auger fine structure of bulk diamond with a gold overlayer after subtracting the overlapping signal.

Another controversial assumption was that the model used in the subtraction assumed a two-dimensional overlayer coverage. For the thermal evaporation of gold on diamond at room temperature, the deposition mode is three dimensional. Thus, the thickness of the gold overlayer, as calculated using a two-dimensional growth model, should be less than the true thickness of the gold islands. However, the gold-overlayer thicknesses on the silicon were determined using the same two-dimensional growth model as described in the experimental section. Since the deposition mode of gold on silicon is three dimensional as well, the equivalent thickness of the gold overlayer was also less than the true thickness of the islands. Therefore, in practice, the signal to be subtracted can be based on the equivalent thicknesses calculated using the two-dimensional model.

Post-deposition annealing was conducted *in vacuo* up to 500 °C. The relative intensity of the gold signal decreased due to the diffusion of gold from the surface into the film presumably through the grain boundaries. However, no change was observed in the peak position and shape of XPS and AES spectra, respectively, indicating very little effect from annealing. This minimal effect of postdeposition annealing was attributed to the inert nature of gold and diamond and the fact that a carbide-forming reaction is not thermodynamically favorable. This result also supports the observation that the *I-V* characteristics remained rectifying after the annealing.

C. Surface pretreatment effects

The metal-semiconductor interface is the most critical region in determination of the electrical properties of metal contacts. For this reason, pretreatments which alter the chemistry or structure of this interface can have a profound effect on the quality of electrical contacts. Thus, several predeposition surface treatments of diamond were examined in this study to evaluate the effects of the typical processes which metal contacts on semiconductors may experience. These were (i) wet chemical cleaning, (ii) vacuum annealing, and (iii) ion bombardment.

The predeposition wet chemical cleaning in a 3:4:1 mixture of sulfuric, nitric, and perchloric acids was intended to remove the nondiamond carbon from the diamond surface. It has been shown that acid cleaning of diamond films affect the *I-V* characteristics of metal contacts.[11,29] This treatment, however, had little effect on the gold-diamond interactions. This meant that the nondiamond carbon on the surface of diamond did not affect the metal-diamond interaction. This conflicts with results reported by Grot *et al.*[11] in which case predeposition cleaning of diamond has a significant influence on the electrical properties of gold contacts. Their gold contacts showed Ohmic and rectifying characteristics on as-grown and chemically cleaned diamond, respectively. The difference was attributed to the presence of residual hydrocarbons on their as-grown diamond surface, which behaved as a current conduction path and increased the leakage current. No such difference was observed in the present study (i.e., gold formed rectifying contacts on

both as-grown and acid cleaned diamond). However, an improvement of the C_{KLL} Auger peak shape (i.e., a relative increase in the intensity of the 259-eV peak) did indicate successful removal of absorbed species from the diamond surface via the acid treatment. It is speculated that the different I-V characteristics are due to lower concentrations of hydrocarbons on the unannealed diamond surfaces in the present study.

Predeposition annealing at ~500 °C was also utilized as a pretreatment of as-grown diamond films. Gold contacts deposited on an annealed diamond film showed rectifying characteristics essentially the same as on the unannealed sample shown in Fig. 1. It was confirmed by XPS that some of the physisorbed oxygen at the surface was desorbed by the predeposition annealing. However, the gold-diamond interaction was not influenced by this treatment. This was reasonable since neither gold nor diamond are inert to oxygen. Since the predeposition annealing was conducted at ~500 °C, it was supposed that the diamond surface remained hydrogen terminated.

The argon sputtering effectively removed the adsorbed species on the surface of diamond. However, at the same time, it induced a damaged layer composed of graphite and amorphous carbon.[13,27,30–32] The I-V characteristics of the gold contacts on these surfaces are shown in Fig. 4. The as-deposited gold contacts were Ohmic in contrast to the case of the nontreated diamond surface. It is speculated that the sputtering created energy states in the band gap of the diamond making the valence band and conduction band essentially continuous. This would cause any metal contact to be Ohmic. Thus, the damaged layer may be useful to obtain as-deposited Ohmic contacts on diamond. However, these Ohmic contacts became rectifying upon annealing as shown in Fig. 4. This change in contact behavior was attributed to the instability of the damaged layer at the diamond surface. It is highly unlikely that this layer reverted back to diamond by the annealing since it appears to contain graphite which is thermodynamically more stable than diamond at the conditions examined. Rather, it is speculated that the damaged layer was absorbed into the gold overlayer upon annealing. The result is a gold contact on nondamaged diamond which was similar to the case shown in Fig. 1.

The damage of the diamond surface by argon sputtering can be confirmed by the broadening of the C 1s peak. The peak broadening is believed to be due to bond-angle distortion and a wider distribution of interatomic distances as has been seen for silicon dioxide by Grunthaner and co-workers.[33] The effect of gold deposition was examined for this surface as well. However, there was no peak-shape change observed due to the presence of gold. The analysis of the C_{KLL} Auger fine structure clearly showed the effect of the argon sputtering on the diamond surface. The surface appeared to be graphitized by the sputtering.[27,30–32] The overlapping peaks from the overlayer were removed in the same manner as for the analysis of the nonsputtered surface. The damaged surface of diamond remained as it was after the gold deposition indicating the lack of interaction between gold and the damaged diamond surface. Thus, it is concluded that

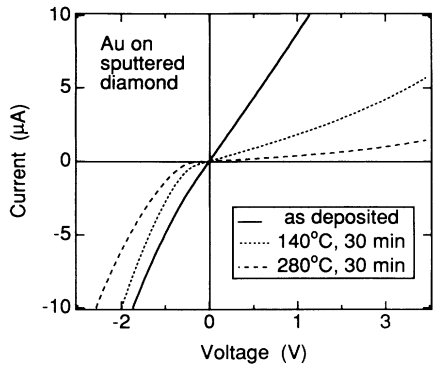

FIG. 4. I-V characteristics of gold contacts on an argon-sputtered surface of boron-doped polycrystalline diamond.

the formation of the as-deposited Ohmic contact on the argon-sputtered surface of diamond was not due to gold-diamond interactions, but rather was due to the modified nature of the diamond surface.

IV. CONCLUSION

It has been shown that interface reactions do not occur between gold contacts and diamond thin films. This is true for both as-deposited and annealed conditions. This is reasonable since "gold carbide" formation is thermodynamically unfavorable. These interface observations correlated well with the rectifying behavior of both the as-deposited and the annealed gold contacts on diamond. The absence of any interface reaction plays a significant role in the determination of the electrical properties of metal contacts on diamond. This will be further emphasized by the results in the following paper.[34]

Various predeposition treatments were also examined. Wet chemical cleaning and predeposition annealing were effective to some extent in removing surface contamination (i.e., nondiamond carbon and absorbed oxygen, respectively), but did not influence the gold-diamond interaction. Argon sputtering produced a damaged, graphiticlike surface and changed the I-V characteristics of the as-deposited gold contacts from rectifying to Ohmic. However, there was still no evidence of gold-diamond interaction on this surface. The lack of interaction was supported by the fact that the I-V characteristics of the gold contacts on the sputtered surface changed from Ohmic to rectifying upon annealing. This change was attributed to the diffusion of the damaged carbon layer into the gold overlayer, resulting in the formation of a gold-undamaged diamond interface.

APPENDIX: SYSTEM DESCRIPTION

The majority of this study utilized an integrated vacuum system (Fig. 5) consisting of a microwave plasma enhanced CVD chamber and an *in vacuo* surface analytical chamber connected via a transfer tube containing a thermal evaporation source for metallization. This vacuum system was designed for the purpose of studying nucleation, growth, metallization, and various aspects of di-

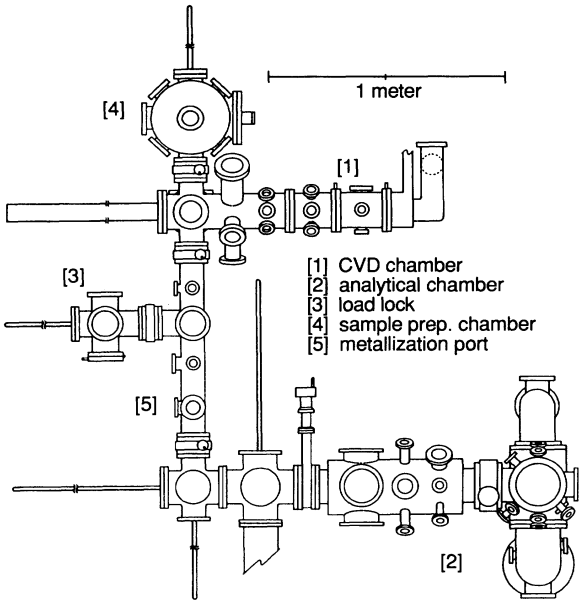

FIG. 5. Schematic of the diamond growth and *in vacuo* surface analysis system used in the present investigation.

amond surfaces without exposing samples to the atmosphere.

The sample preparation chamber, isolated from the growth chamber by a gate valve, is adjacent to the growth chamber. It is possible to heat the substrate up to 500 °C in various atmospheres, including vacuum, as well as to clean the substrate *in vacuo* by ion bombardment in this chamber. The base pressure of this chamber is kept below 1×10^{-8} Torr by a turbomolecular pump.

Diamond films are grown in the main growth chamber. The plasma is created from the energy supplied by an ASTEX 1-kW microwave source (2.45 GHz). A heater is attached to the back side of the molybdenum substrate holder. Both the microwave power and the substrate heater are used to control the substrate temperature which is monitored by an infrared pyrometer. Thus the substrate temperature may be varied independently of the microwave power. As a consequence it is possible to grow diamond films in both immersed and downstream modes. The pressure and flow rates are controlled and monitored by MKS pressure and mass-flow controllers, respectively. A station for reflection high-energy electron diffraction (RHEED) is attached to this chamber to observe the surface structure of grown films. During diamond growth the chamber is pumped by a roots blower system and the base pressure of this chamber is maintained in the 10^{-8}-Torr range by a turbomolecular pump. An *in situ* laser reflectance interferometry is used to measure growth rates of the films during deposition.[35] As previously discussed, for the present work, diamond films were not grown in this system but rather were grown in a separate microwave CVD apparatus and introduced to the metallization stage via the load lock chamber attached to the transfer tube.

The multitechnique analytical chamber constitutes the other main half of the integrated vacuum system. It is pumped by an ion pump and a titanium sublimation pump to a base pressure of 1×10^{-10} Torr. A magnesium-aluminum dual anode, nonmonochromatized soft-x-ray source is used for XPS. The data are collected by a pulse counter. An electron-beam gun is operated with a typical incident energy at 3 keV for AES. The data are collected either by a pulse counter for the direct mode or by a lock-in amplifier combined with an 8-kHz modulation at 6-V peak to peak for the differentiated mode. Both techniques share a common RIBER MAC2 semi-imaging-type electron energy analyzer system, featuring the combination of high transmission and high luminosity.[23] A sample heater and a sputtering gun are also available in the analytical chamber. There is also a reverse view, low-energy-electron-diffraction (LEED) optics with a phosphorus screen and a setup for electron-simulated desorption (ESD) with a quadrupole mass analyzer and an electron gun.

The load lock is attached to the transfer tube which connects the growth chamber and the analytical chamber. Two gate valves terminate both ends of the transfer tube. An ion pump as well as a titanium sublimation pump are used to maintain the vacuum of the transfer tube at less than 1×10^{-8} Torr. On this transfer tube there is a resistive heating-type evaporation source for the metal deposition used in this study as discussed in the experimental section.

[1]J. F. Prins, Appl. Phys. Lett. **41**, 950 (1982).
[2]M. W. Geis, D. D. Rathman, D. J. Ehrlich, R. A. Murphy, and W. T. Lindley, IEEE Electron Device Lett. **8**, 341 (1987).
[3]H. Shiomi, Y. Nishibayashi, and N. Fujimori, Jpn. J. Appl. Phys. **28**, L2153 (1989).
[4]H. Shiomi, Y. Nishibayashi, and N. Fujimori, Jpn. J. Appl. Phys. **29**, L2163 (1990).
[5]M. D. Bell and W. J. Leivo, Phys. Rev. **111**, 1227 (1958).
[6]G. H. Glover, Solid-State Electron. **16**, 973 (1973).
[7]C. A. Mead and T. C. McGill, Phys. Lett. **58A**, 249 (1976).
[8]F. J. Himpsel, P. Heimann, and D. E. Eastman, Solid State Commun. **36**, 631 (1980).
[9]G. Sh. Gildenblat, S. A. Grot, C. W. Hatfield, A. R. Badzian, and T. Badzian, IEEE Electron Device Lett. **11**, 371 (1990).
[10]G. Sh. Gildenblat, S. A. Grot, C. R. Wronski, A. R. Badzian, and T. Badzian, Appl. Phys. Lett. **53**, 586 (1988).
[11]S. A. Grot, G. Sh. Gildenblat, C. W. Hatfield, C. R. Wronski, A. R. Badzian, T. Badzian, and R. Messier, IEEE Electron Device Lett. **11**, 100 (1990).
[12]See, for example, A. T. Collins, E. C. Lightowlers, and A. W. S. Williams, Diamond Res. (Suppl. Indust. Diamond Rev.) **30**, 19 (1970), and references therein.
[13]S. Sato and M. Iwaki, Nucl. Instrum. Methods B **32**, 145 (1988).
[14]J. F. Prins, J. Phys. D **22**, 1562 (1989).
[15]K. L. Moazed, R. Nguyen, and J. R. Zeidler, IEEE Electron Device Lett. **9**, 350 (1988).
[16]K. L. Moazed, J. R. Zeidler, and M. J. Taylor, J. Appl. Phys. **68**, 2246 (1990).
[17]D. Narducci, J. J. Cuomo, C. R. Guarnieri, and S. J.

Whitehair, in *Diamond, Silicon Carbide and Related Wide Bandgap Semiconductors,* edited by J. T. Glass, R. Messier, and N. Fujimori, MRS Symposia Proceedings No. 162 (Materials Research Society, Pittsburgh, 1990), pp. 333–339.
[18]H. Shiomi, H. Nakahata, T. Imai, Y. Nishibayashi, and N. Fujimori, Jpn. J. Appl. Phys. **28**, 758 (1989).
[19]L. J. Brillson, J. Vac. Sci. Technol. **20**, 652 (1982).
[20]L. J. Brillson, Surf. Sci. Rep. **2**, 123 (1982).
[21]K. Kobashi, K. Nishimura, Y. Kawate, and T. Horiuchi, Phys. Rev. B **38**, 4067 (1988).
[22]C. S. Fadley, R. J. Baird, W. Siekhaus, T. Novakov, and S. Å. L. Bergström, J. Electron. Spectrosc. **4**, 93 (1974).
[23]P. Staib and U. Dinklage, J. Phys. E **10**, 914 (1977).
[24]M. G. Mason, Phys. Rev. B **27**, 748 (1983).
[25]F. R. McFeely, S. P. Kowalczyk, L. Ley, R. G. Cavell, R. A. Pollak, and D. A. Shirley, Phys. Rev. B **9**, 5268 (1974).
[26]D. N. Belton and S. J. Schmieg, J. Vac. Sci. Technol. A **8**, 2353 (1990).
[27]P. G. Lurie and J. M. Wilson, Surf. Sci. **65**, 476 (1977).
[28]These spectra were taken from a bulk diamond sample placed next to the polycrystalline sample throughout the deposition. This bulk diamond was used to obtain a flat diamond surface for the spectra subtraction. There was essentially no difference between these peaks and those obtained from the polycrystalline sample.
[29]Y. Mori, H. Kawarada, and A. Hiraki, Appl. Phys. Lett. **58**, 940 (1991).
[30]B. E. Williams and J. T. Glass, J. Mater. Res. **4**, 373 (1989).
[31]A. Hoffman, P. J. K. Paterson, and S. Prawer, Nucl. Instrum. Methods B **52**, 63 (1990).
[32]Y. Cong, R. W. Collins, R. Messier, K. Vedam, G. F. Epps, and H. Windischmann, J. Vac. Sci. Technol. A **9**, 1123 (1991).
[33]F. J. Grunthaner, P. J. Grunthaner, R. P. Vasquez, B. F. Lewis, J. Maserjian, and A. Madhukar, J. Vac. Sci. Technol. **16**, 1443 (1979).
[34]T. Tachibana, B. E. Williams, and J. T. Glass, following paper, Phys. Rev. B **45**, 11 975 (1992).
[35]B. R. Stoner, B. E. Williams, S. D. Wolter, K. Nishimura, and J. T. Glass, J. Mater. Res. **7**, 257 (1992).